

# Construction of White-Light-Emitting Silk Protein Hybrid Films by Molecular Recognized Assembly among Hierarchical Structures

Naibo Lin, Fan Hu, Yilin Sun, Chenxu Wu, Hongyao Xu,\* and Xiang Yang Liu\*

The fabrication of bio-hybrid functional films is demonstrated by applying a materials assembly technique. Based on the hierarchical structures of silk fibroin materials, functional molecular/materials, i.e., quantum dots (QDs), can be fixed to amino acid groups in silk fibroin films. It follows that white-light-emitting QD silk hybrid films are obtained by hydrogen bond molecular recognition to the  $\text{-COO}^-$  groups functionalized to blue luminescent ZnSe (5.2 nm) and yellow luminescent CdTe (4.1 nm) QDs in a molar ratio of 30:1 of ZnSe to CdTe QDs. Simultaneously, a systematic blue shift in the emission peak is observed from the QD solution to QDs silk fibroin films. The significant blue shift hints the appearance of the strong interaction between QDs and silk fibroins, which causes strong white-light-emitting uniform silk films. The molecular recognized interactions are confirmed by high resolution transmission electron microscopy, field scanning electron microscope, and attenuated total internal reflectance Fourier transform infrared spectroscopy. The QD silk films show unique advantages, including simple preparation, tunable white-light emission, easy manipulation, and low fabrication costs, which make it a promising candidate for multicomponent optodevices.

new materials become particularly important. In this regard, the focus of research in materials science has been devoted to the three categories: ultra-performance materials, multifunctional materials and smart and responsive materials.<sup>[1]</sup> Due to the exhaustion of crude oils in the years to come, biopolymers will become increasingly important as renewable and sustainable materials.<sup>[2]</sup> *Bombyx mori* silk, as one of biopolymers, has recently emerged as one of the highly promising candidates owing to its availableness, excellent mechanical and optical properties.<sup>[3]</sup> In addition to its traditional use in textile industries, *Bombyx mori* silk fibroins have been found various applications in microfluidic device, bone-like resorbable scaffolds, biocompatible optical/electrical devices and bioimaging, once silk fibroins were fabricated into a special form or functionalized by particular molecules.<sup>[4]</sup>

It is very desirable to develop a general approach to functionalize soft materials, such as silk proteins. It is the aim of this paper to put forward the idea of Materials Assembly in the functionalization of soft materials. In this context, we will take *Bombyx mori* silk fibroin as an example to functionalize silk fibroin films using quantum dots (QDs), and expected to combine the advantages of both QDs and silk fibroin materials.

Quantum dots have been investigated extensively in the last two decades because of their premium white-light-emitting efficiency and photostability in photonic devices.<sup>[5]</sup> It is well known that QD aqueous solutions are chromophores and possess numerous advantages, i.e., high-fluorescence quantum efficiency, good photostability, low fabrication costs, and chemical flexibility.<sup>[6]</sup> White-light-emitting materials can be achieved by doping polymeric host materials using fluorescent QDs, or by subsequent deposition of individual emitter layers leading to stacked multilayer arrangements.<sup>[7]</sup> White-light-emitting protein films and devices using protein nanowires (amyloid fibrils) as structural templates are useful for future organic electronics and multicomponent optodevices.<sup>[8]</sup> However, to the best of our knowledge, white-light-emitting silk materials have never fabricated.

We will take advantage of Materials Assembly to solve the challenge of aggregation of QDs. This helps to harmonize QDs

## 1. Introduction

The research and engineering of materials have become one of the most exciting areas across physics, chemistry, biology and engineering. In addressing the current issues concerning health, environment and the sustainability of development,

Dr. N. B. Lin, F. Hu, Y. L. Sun, Prof. C. X. Wu,  
Prof. X. Y. Liu  
Research Institute for Biomimetics and Soft Matter  
College of Materials & Department of Physics  
Xiamen University  
Xiamen 361005, China  
E-mail: phyliuxy@nus.edu.sg

Dr. N. B. Lin, Prof. H. Y. Xu, Prof. X. Y. Liu  
College of Material Science and Engineering & State Key Laboratory for  
Modification of Chemical Fibers and Polymer Materials  
Donghua University  
Shanghai 201620, China  
E-mail: hongyaoxu@dhu.edu.cn

Dr. N. B. Lin, Prof. X. Y. Liu  
Department of Physics  
National University of Singapore  
2 Science Drive 3, 117542, Singapore



DOI: 10.1002/adfm.201400249

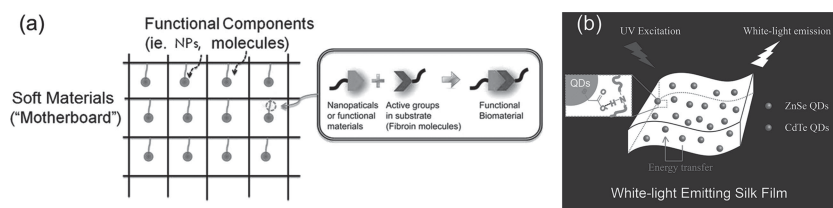
with *Bombyx mori* silk in the hybrid materials, which will make QDs homogeneously incorporate into the bulk of silk materials. In addition, by mixing blue luminescent ZnSe and yellow luminescent CdTe QDs, we can produce white-light-emitting biopolymer/QD hybrid materials with various color temperatures. It is worth noting that uniform QD/silk fibroin hybrid films can be obtained from the conventional aqueous solution based drop-casting process under a “green” condition. The uniform hybrid film processing can even be extended to roll-coating (with directional solvent evaporation) and ink-jet printing (i.e., controlled drop-casting), which are inevitably required for the fabrication of large-area films.<sup>[9]</sup>

## 2. Results and Discussion

### 2.1. Principle and Strategy of Materials Assembly

As mentioned, the key idea of Materials Assembly is to functionalize soft materials by fixing some functional components (i.e., functional molecules or nanomaterials) to some specific points of the networks of soft materials. After assembly, the soft materials should on one hand maintain the original properties of the materials and on the other hand acquire some additional properties.

In order to achieve this functionalization, two factors to be considered in this process are as follows: there should be sufficiently large mesh sizes in the soft materials (“motherboard”) to accommodate functional components; the functional components should be able to recognize some specific functional groups in the meshes of soft materials, so that they can be recognized and fixed to the soft materials (Scheme 1a). If the functional components can't be recognized in the original state, some functional groups should be prefixed (functionalized) to the surfaces to make them recognizable by the meshes of soft materials. *Bombyx mori* silk fibroin will be adopted for the functionalization in this work as the bulk material, the primary structure of silkworm silk proteins is composed of repetitive sequences that can be divided into small blocks (Figure 1).<sup>[10a]</sup>



**Scheme 1.** (a) Strategy of construction of bio/nano hybrid materials by Materials Assembly. (b) Schematic illustration of the structure of white-light-emitting silk films and the creation of white photoluminescence.

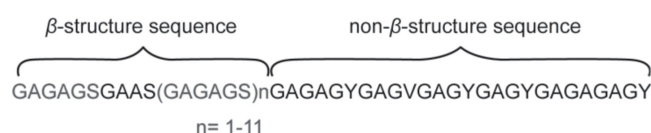
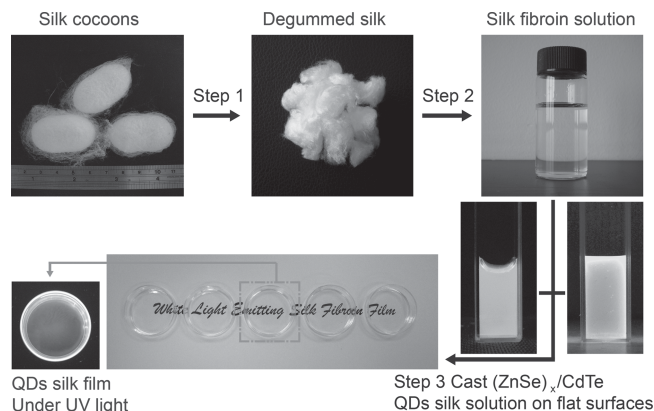


**Figure 1.** The primary structure of silkworm silk proteins.



**Scheme 2.** Illustration of the preparation of quantum dots (QDs) functionalized white-light-emitting silk fibroin films.

*Bombyx mori* silk fibroin is composed of light- and heavy-chains linked by disulfide bond. The regular sequence of the heavy-chain is associated with the crystalline regions in silk.<sup>[11]</sup> The amino acid sequence in the crystalline region is considered to be (GAGAGS)<sub>n</sub> and the sequence in the amorphous region contains Tyr-rich domains. Both the silk fibers and the regenerated silk materials such as sponge and film consist of a molecular network structure. The meshes are in principle sufficiently large to accommodate various QDs.<sup>[12]</sup>

To achieve Materials Assembly with the NH groups in silk fibroin chains, QDs need to be functionalized. QDs, namely, ZnSe and CdTe, were synthesized by hydrothermal technologies.<sup>[13]</sup> For more details, see the Experimental Section. In the synthesis of QDs, 3-mercaptopropionic acid was added to the system. This is not only to stabilize the QDs, but also to functionalize the surface of the QDs with carboxy groups for the above mentioned Materials Assembly. We notice that NH groups are distributed in the silk fibroin chains. Because of NH groups and carboxy groups in the silk fibroin network, the QDs can homogeneously distribute in silk fibroin molecules.

### 2.2. Preparation of White-Light-Emitting Silk Films

In this study, the functionalized blue-light emission ZnSe and the yellow-light emission CdTe QDs were synthesized. To create the white emission, the blue- and yellow-light emission balance should be acquired, which is to be achieved by tuning the molar ratio of the mixed ZnSe and CdTe QDs (c.f. Scheme 1b). Meanwhile, regenerated silk fibroin solutions should be prepared as illustrated by

**Scheme 2.** The preparation should begin with the purification of *Bombyx mori* cocoons, which includes removing sericin, dissolving silk fibers by LiBr solutions, extracting LiBr salt by dialysis, centrifugation and microfiltration, and concentrating the aqueous silk solutions. Fixing QDs into the NH groups in silk fibroin films starts from step 3. The QDs functionalized silk

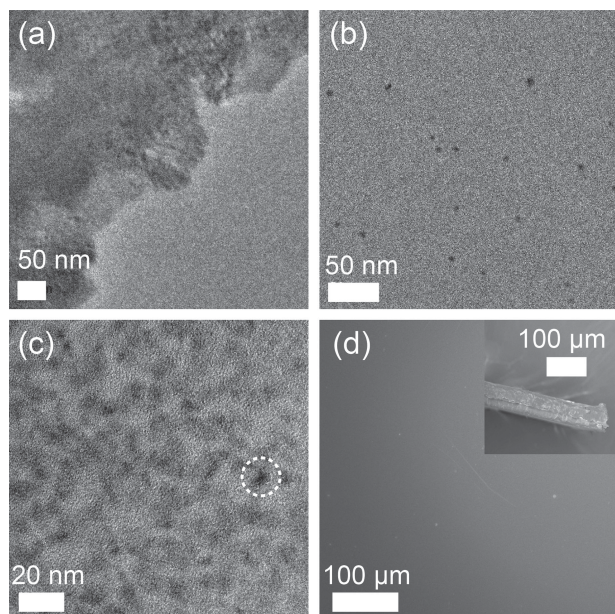


**Figure 2.** The high resolution transmission electron microscopic images (HRTEM), (a) Aggregated (ZnSe)<sub>30</sub>/CdTe QDs fished out from an (ZnSe)<sub>30</sub>/CdTe QD aqueous solution kept at room temperature for one week, (b) Uniform distribution of CdTe QDs in a transparent ultrathin silk film sample (50–70 nm), (c) (ZnSe)<sub>30</sub>/CdTe silk fibroin film, the black point in the circle is CdTe QDs. (d) Field emission scanning electron microscope (FESEM) images of a (ZnSe)<sub>30</sub>/CdTe silk fibroin film. Inset: the cross section image. The thickness of the film is about 63 μm.

fibroin solution was cast onto the surface of a polystyrene Petri dish. See the Experimental Section for more details.

### 2.3. Structural Characterization and the Mechanism of Materials Assembly

ZnSe, (ZnSe)<sub>x</sub>/CdTe, and CdTe QDs were characterized by a high resolution transmission electron microscope (HRTEM, JEM-3010F, JEOL, Japan). After one week, (ZnSe)<sub>30</sub>/CdTe QDs aggregate as commonly observed in aqueous solutions at room temperature (c.f. Figure 2a). On the other hand, from Figure 2b, the HRTEM image displays that functionalized CdTe QDs are uniformly distributed in the silk fibroin films. Moreover, the CdTe QDs (black points) in silk films are spherical with a diameter of ~4.1 nm. Figure 2c shows the presence of the (ZnSe)<sub>30</sub>/CdTe QDs in silk films, ZnSe QDs appear as some floc points with a diameter in ca. 5.2 nm. The uniform dispersion of QDs can be attributed to the hydrogen bond interaction between QDs and the silk fibroin molecules. From field emission scanning electron microscopy (FESEM) (Figure 3d), it can be seen that the (ZnSe)<sub>30</sub>/CdTe QD silk film surface is smooth and the thickness of the film is about 63 μm.

As mentioned before, to achieve the uniform dispersion of QDs in silk fibroin films, 3-mercaptopropionic acid was used to modify QDs to obtain the functionalized QDs with carboxy groups. To characterize the interaction between the QDs and silk fibroin, pure silk film and concentrated QD silk film were prepared in a similar procedure illustrated by Scheme 2 for

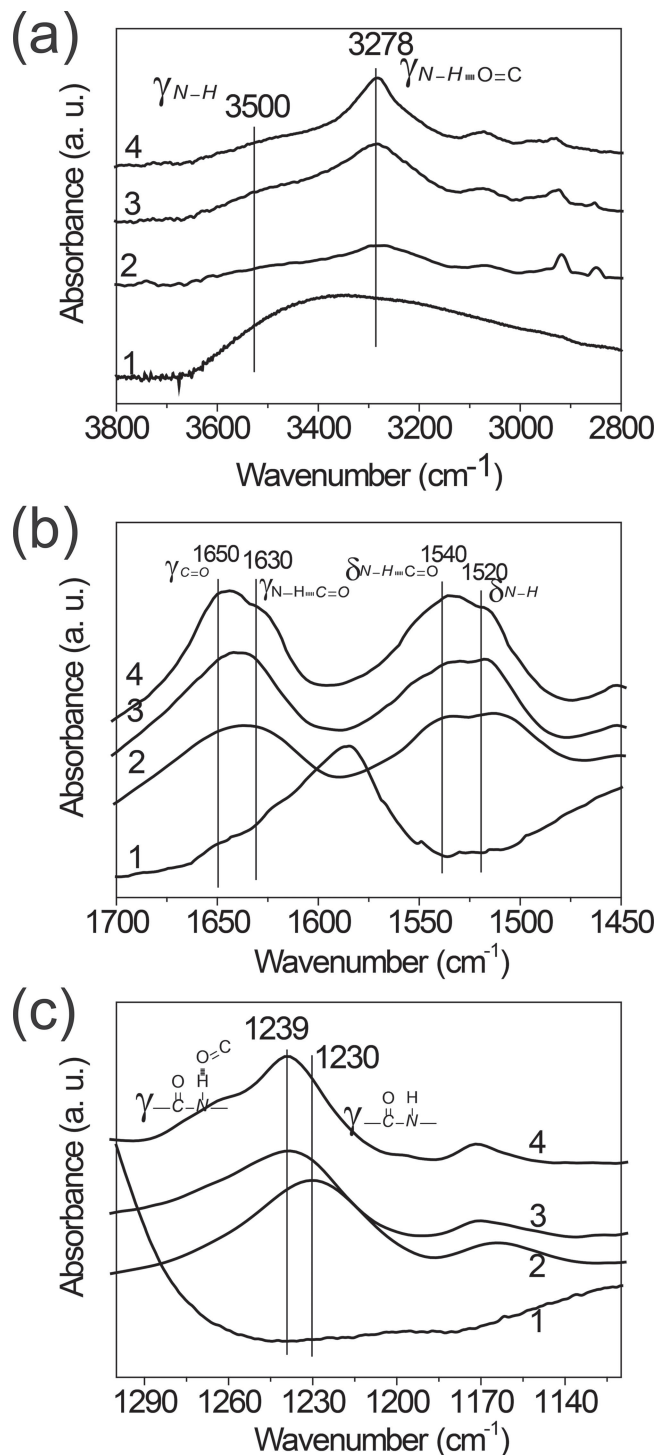


**Figure 3.** Expanded FTIR spectra recorded in the region of (a) 3800–3000 cm<sup>-1</sup> (b) 1700–1450 cm<sup>-1</sup> and (c) 1300–1120 cm<sup>-1</sup> for (1) the (ZnSe)<sub>30</sub>/CdTe QD powder, (2) the pure silk films, (3) (ZnSe)<sub>30</sub>/CdTe composite films, and (4) high (ZnSe)<sub>30</sub>/CdTe concentration composite films.

comparison. 0.5 mL silk fibroin solution was mixed with a 5 mL sodium hydroxide solution to form pure silk film. For high concentration QD silk film, it was obtained from the mixture of 0.5 mL silk fibroin solution and 5 mL (ZnSe)<sub>30</sub>/CdTe QD solution. As we



known, pH dramatically affects the molecular interaction and fluorescence property of the QDs.<sup>[14]</sup> In order to keep molecular interactions of the films with different concentrations of QDs comparable and maintain high fluorescence efficiency, the pH of the all mixture solutions was tuned to 8.1 by hydrochloric acid before concentrating. Notice that the isoelectric point (pI) of amphoteric polyelectrolyte silk fibroin molecules is 3.8–3.9.<sup>[15]</sup> Above the pI, the silk fibroin chain should be negatively charged at side chain. This rules out the possibility of the charge–charge attraction of other groups of silk fibroin molecules with the carboxylic groups (COO<sup>−</sup>) on the surface of QDs.

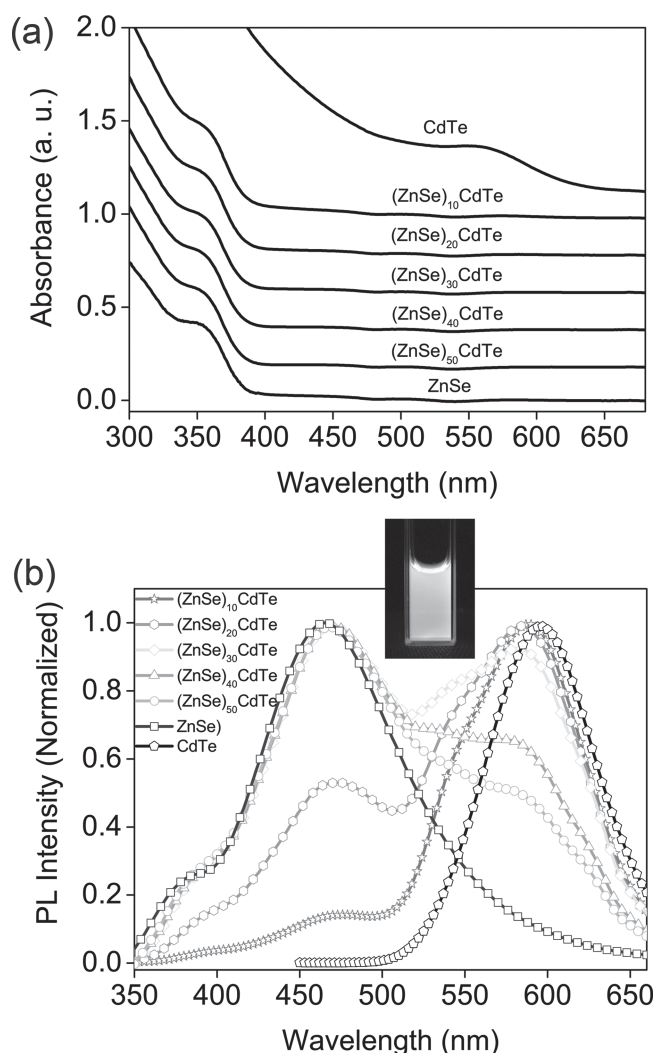
Fourier transform infrared spectroscopy (FTIR) is one of the main tools for the study of the hydrogen-bond interaction in organic/inorganic materials.<sup>[16]</sup> FTIR absorption changes, in terms of strength and positions of characteristic functional groups, are attributed to the existence of specific intermolecular and/or intramolecular interactions. Therefore, we use FTIR spectra of these compounds to elucidate the mechanism of Materials Assembly between the silk fibroin and QDs. Total reflection-Fourier transform infrared (ATR-FTIR) spectroscopic patterns of a (ZnSe)<sub>30</sub>CdTe QD powder, the pure silk films, (ZnSe)<sub>30</sub>CdTe composite films, and high (ZnSe)<sub>30</sub>CdTe concentration composite films were obtained. (ZnSe)<sub>30</sub>/CdTe solid powder was taken by evaporation of the QD solution at 60 °C. It can be observed from Figure 3a that the stretching vibration peak of free amino (NH) group silk films located at 3500 cm<sup>−1</sup> and hydrogen bonded amino groups located at 3278 cm<sup>−1</sup>. The strength of hydrogen bonded amino groups is significantly enhanced and the peak area increased as the QD content is increased in the silk film. Due to the same preparation process of the pure silk film and QD hybrid silk film, any change in the FTIR spectra in this region is attributed to the change in the chemical environments of the amino groups, especially the formation of hydrogen bonds. Therefore, the hydrogen-bonding between the carboxylic groups (COO<sup>−</sup>) of QDs and the amino groups of silk fibroin must be crucial in establishing the interactions between silk fibroin and QDs in the final structure of the white-light-emitting nanocomposite. For (ZnSe)<sub>30</sub>CdTe QD powder, there is strong characteristic absorption band, attributed to the hydroxyl vibrations, no stretching vibration peak of amino group can be observed.

Figure 3b shows a red shift of the infrared spectra in the region of 1450–1700 cm<sup>−1</sup> for (ZnSe)<sub>30</sub>CdTe QD powder, the pure silk films, (ZnSe)<sub>30</sub>CdTe composite films, and ZnSe)<sub>30</sub>CdTe concentrated composite films. It can be seen that the silk protein materials show the characteristic vibrational bands at 1630–1650 cm<sup>−1</sup> for amide I (C=O stretching) and at 1540–1520 cm<sup>−1</sup> for amide II (secondary NH bending) in the FTIR spectrum.<sup>[42]</sup> From the FTIR profile of (ZnSe)<sub>30</sub>CdTe QD powder, it can be seen that carbonyl (C=O) stretching vibration peak from COO<sup>−</sup> located at 1585 cm<sup>−1</sup>. Meanwhile, the hydrogen bonded carbonyl (C=O) stretching vibration peak located at 1630 cm<sup>−1</sup> become strong when the content of QDs in silk film rises. This can be assigned to the existence of massive COO<sup>−</sup> from the QD surface. The establishment of hydrogen bonds between the carboxylic groups and the amino groups also can be proved by bending vibration of amino group in FTIR. The stronger characteristic absorption band at 1540 cm<sup>−1</sup>, which may be attributed to the more bending vibration of bonded amino group resulted from hydrogen

bond interaction between the NH and COO<sup>−</sup> (c.f. Figure 3b). Simultaneously, the C–N stretching vibration absorption band intensity also shifts from 1230 cm<sup>−1</sup> to 1239 cm<sup>−1</sup> (Figure 3c), when the content of QDs in silk film rises. These indicate that there is stronger hydrogen bond interaction in QD silk film than in pure silk film. This is consistent with the FTIR absorption spectra of N–H stretching/blending vibration absorption band and also further supports that the hydrogen-bonding between the carboxylic group of QDs and the amino group of silk fibroin is crucial in establishing the interactions between silk fibroin and QDs in the final structure of the white-light-emitting nanocomposite.

#### 2.4. Optical Characteristics of White-Light-Emitting Silk–QD Hybrid Films

Figure 4b shows the fluorescence emission spectra of the ZnSe, (ZnSe)<sub>x</sub>/CdTe composites, and CdTe QDs excited at 330 nm.



**Figure 4.** (a) UV-vis absorption spectra, and (b) normalized fluorescence spectra of CdTe, (ZnSe)<sub>x</sub>CdTe and ZnSe QD solutions. Inset: Image of (ZnSe)<sub>30</sub>CdTe QD aqueous solutions under UV light (302 nm).

The spectra were normalized at their peak wavelengths. The  $(\text{ZnSe})_{50}/\text{CdTe}$  QD composites have a slight bluish tinge. After decreasing the molar ratio from 50:1 to 30:1,  $(\text{ZnSe})_{30}/\text{CdTe}$  QD composites appear bright white. When the ratio of ZnSe to CdTe QDs is 20:1, the  $(\text{ZnSe})_{20}/\text{CdTe}$  QD composites display an orange tinge. When further decreasing the feed ratio to 10:1, the QD composites exhibit orange. Therefore, the control of these  $(\text{ZnSe})_x/\text{CdTe}$  QD mixtures enables us to balance the relative strength of the orange and blue components in the white light emission. The optimized blend with relative molar concentration ZnSe/CdTe QDs of 30:1, which will result in white emission with Commission Internationale d'Eclairage (CIE) coordinates (0.31, 0.34). Comparing the  $(\text{ZnSe})_{30}/\text{CdTe}$  QD emission with the different color temperatures (warm, cold, and pure white) of commercial white-light LEDs, we can conclude that the emission belonged in the cold-white-light classification.

Figure 5 shows UV-vis absorption spectra and fluorescence spectra of CdTe,  $(\text{ZnSe})_x/\text{CdTe}$  and ZnSe QD silk fibroin films. It follows that all silk ZnSe,  $(\text{ZnSe})_x/\text{CdTe}$ , and CdTe QD films show homogeneous photophysical properties. The linear transmittance of the films is above 90% within the range of visible light (c.f. Scheme 1). The respective UV-vis absorption spectrum of  $(\text{ZnSe})_x/\text{CdTe}$  silk composite films in Figure 5a, for example, the absorbance edge, is similar to that in aqueous solutions, indicating that the 1s–1s electronic transitions of QDs are almost unaffected after QDs were doped into the silk fibroin film.<sup>[17]</sup>

The ZnSe/CdTe/silk fibroin composite films exhibited tunable luminescent properties, and the best chromaticity with coordinates of (0.33, 0.37) when the feed ratio of ZnSe and CdTe QDs were 30:1, demonstrating its potential applications in full-color display devices. Figure 5b shows the fluorescence emission spectra of a series of ZnSe QD silk film,  $(\text{ZnSe})_x/\text{CdTe}$  QD silk film, and CdTe QD silk. As expected, the fluorescence emission spectra of the QD silk films resemble that of the QD aqueous solutions, and so do the absorption spectra. In addition, with increasing content of CdTe QDs in the silk fibroin films, the relative emission intensity from ZnSe QDs decreased, while incorporating QDs into silk fibroin films slightly alters the optical properties of silk fibroin films. From Figure 3c, it can be observed that a systematic blue shift in the band edge emission peak occurs when the  $(\text{ZnSe})_{20}/\text{CdTe}$  were incorporated into silk fibroin films. This indicates the strong interactions between silk fibroin molecules and the QDs. The interactions avoid the aggregation of QDs when they are incorporated into silk fibroin films.

We notice that the fluorescence spectra of  $(\text{ZnSe})_{10}/\text{CdTe}$  QD silk composites show that the intensity of the reddish yellow peak is stronger than that of the blue, although the amount of the incorporated CdTe QDs unit is lower than that of the ZnSe QDs. This may be attributed to the energy transfer from ZnSe QDs to CdTe QDs. Experimentally, it can be found that the fluorescence emission maxima of ZnSe QDs is at 397 nm, corresponding to the excited peaks of CdTe QDs. This implies that the Förster energy transfer from ZnSe QDs to CdTe QDs can happen. This is in agreement with the work of Bawendi and co-workers,<sup>[18]</sup> in which the spectroscopic evidence of energy transfer in

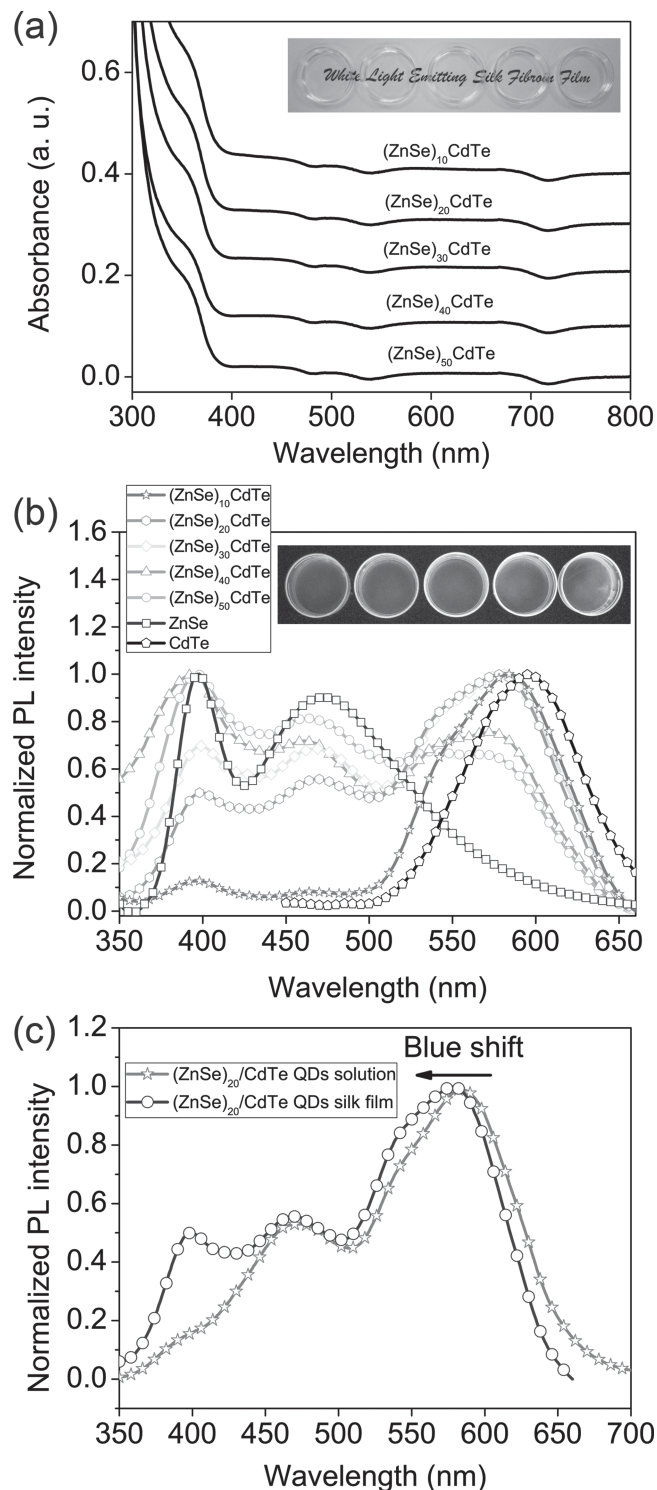


**Figure 5.** (a) UV-vis absorption spectra and (b) normalized fluorescence spectra of CdTe,  $(\text{ZnSe})_x/\text{CdTe}$  and ZnSe QD silk fibroin films. Images of  $(\text{ZnSe})_x/\text{CdTe}$  QD silk film under normal light (Inset a) and 302 nm UV light (Inset b). (c) Normalized fluorescence spectra of  $(\text{ZnSe})_{20}/\text{CdTe}$  aqueous solution and silk film.

close-packed CdSe QD solids due to dipole–dipole inter-dot interactions between proximal dots has been demonstrated. The fluorescence quantum yield value of the  $(\text{ZnSe})_{30}/\text{CdTe}$

QD silk film was measured at exciting light 360 nm, which is 4.06%.

### 3. Conclusions

A series of  $(\text{ZnSe})_x/\text{CdTe}$  QD solutions have been mixed with various molar ratios of ZnSe QDs and CdTe QDs. These composite QD solutions are combined into silk fibroin films by a drop-casting method using a Material Assembly. SEM and high-resolution TEM images show the films have very smooth surfaces and the narrowly distributed  $(\text{ZnSe})_x/\text{CdTe}$  QDs are evenly dispersed. By changing the molar ratios of  $(\text{ZnSe})_x/\text{CdTe}$  QDs in silk fibroin films, functionalized silk films with tunable luminescence porosities can be achieved. Fortunately, we can balance the strength of the relative blue and yellow light emissions, thereby attaining white-light-emitting QDs. It is proved that the strong interaction by the hydrogen bonds between QDs and fibroin results in the homogenous distribution of QDs in silk film. The strategy of molecular recognition is not only limited between the  $(\text{ZnSe})_x/\text{CdTe}$  QDs and silk protein, but can be applied to other materials, such as between non-toxic quantum dots and other biomaterials. Our research may allow a novel and efficient route toward developing white-light-emitting biomaterials. The development of white-light-emitting biomaterials will break the traditional ideas using conjugated organic materials as a luminescent layer, and pave the way for fabricating advanced optical devices, such as biodegradable capsule endoscopes.

### 4. Experimental Section

**Materials:** All chemicals are of analytical grade and used as received without further purification. Mercaptopropionic acid (MPA,  $\text{HSCH}_2\text{CH}_2\text{CO}_2\text{H}$ ), tellurium powder (Te, ~200 mesh), selenium powder (Se, ~200 mesh), cadmium sulfate ( $\text{CdSO}_4 \cdot 8/3 \text{ H}_2\text{O}$ ), zinc nitrate ( $\text{Zn(NO}_3)_2 \cdot 6 \text{ H}_2\text{O}$ ), sodium borohydride ( $\text{NaBH}_4$ ), sodium bicarbonate ( $\text{NaHCO}_3$ ), and lithium bromide (LiBr) were obtained from Aldrich Chemical Company. The silk cocoons were obtained from NO. 2 Liangguang *Bombyx mori* silkworm raised on a diet of Silkworm Chow. The water used in all experiments is ultra-pure (the resistivity  $>18 \text{ M}\Omega \text{ cm}^{-1}$ ).

**Synthesis of ZnSe QDs:** Sodium hydrogen selenium ( $\text{NaHSe}$ ) was produced in an aqueous solution by the reaction of sodium borohydride ( $\text{NaBH}_4$ ) with tellurium powder at a molar ratio of 2:1 at first. Then freshly synthesized oxygen-free  $\text{NaHSe}$  solution was mixed with nitrogen-saturated  $1.25 \times 10^{-3} \text{ mol L}^{-1} \text{ Zn(NO}_3)_2$  aqueous solution at  $\text{pH} = 10.0$ , and with MPA as a stabilizing agent. The molar ratio of  $\text{Zn}^{2+}:\text{MPA}:\text{Se}^{2-}$  was fixed at 1:2.4:0.5. The ZnSe precursor solution was put into a Teflon-lined stainless steel autoclave with a volume of 20 mL. The autoclave was maintained at the reaction temperature  $180^\circ\text{C}$  for 45 min and then cooled to room temperature by a hydrocooling process.

**Synthesis of CdTe QDs:** Aqueous CdTe QDs solutions were synthesized by the same procedure and molar ratio as above from intermediary-sodium hydrogen telluride ( $\text{NaHTe}$ ) and cadmium sulfate at  $\text{pH} = 11.4$ .<sup>[13]</sup> CdTe QDs were obtained by the hydrothermal process using 20 mL autoclave at  $180^\circ\text{C}$  for 40 min.

**Silk Fibroin Solution:** The preparation of silk fibroin solution begins with the purification of *Bombyx mori* cocoons by removing sericin in 0.05% (w/v)  $\text{NaHCO}_3$  for 50 min and then rinsing thoroughly with deionization (DI) water.<sup>[19]</sup> Upon completion of this step, dry silk fibers were dissolved in 9.3 M LiBr solution at  $40^\circ\text{C}$ . The LiBr salt is

then extracted using a dialysis cassette for 48 h and the remaining impurities in fibroin solution are removed through centrifugation and microfiltration. The final concentration of aqueous silk solution was ~8.0 wt%, determined by weighing method.

**White-Light-Emitting Silk Fibroin Film:** ZnSe and CdTe QDs solutions were mixed by volume ratio (equal to molar ratio) 10:1~50:1. For the typical preparation (c.f. Scheme 1), 0.5 mL silk fibroin solution was then blended with 2 mL  $(\text{ZnSe})_x/\text{CdTe}$  QD solution, oscillated for 5 min. QDs/fibroin hybrid solutions were cast on polystyrene substrates and dried at  $25^\circ\text{C}$  with humidity 30% until all the solvent had evaporated to give solid silk fibroin films. The prepared samples were then carefully removed by loosening at one corner of the master and subsequent levering-off using a thin razor blade to obtain freestanding films.

**Instruments:** The FTIR spectra of silk fibers were recorded on a Thermo Nicolet 5700 spectrometer by attenuated total reflection-Fourier transform infrared (ATR-FTIR) spectroscopy. Absorption spectra were recorded with an UV-vis Varian Cary 50 Bio spectrometer. Fluorescence spectra were measured with Varian Cary Eclipse spectrometer. Fluorescence quantum yield was recorded on a JASCO FP-6600 spectrophotometer using an integrating sphere (ISF-513). The mean diameter and morphology of QDs were characterized by high resolution transmission electron microscopy (HRTEM, JEM-3010F, JEOL, Japan). Field emission scanning electron microscopes were recorded on a JEOL JSM-6700F field electron microscope operating at 5 kV.

### Acknowledgements

This work is financially supported by AcRF Tier 1 (R-143-000-497-112), National Nature Science Foundation (Nos. 21271040, 51073031), the Excellent Young Teachers Training Program of Shanghai (ZZyyy12001), Shanghai Institute of Technology Scientific Research Foundation for Introduced Talent (YJ2012-25) and Fundamental Research Funds for the Central Universities (ZK1018).

Received: January 23, 2014

Revised: April 3, 2014

Published online: June 24, 2014

- [1] a) X. Y. Liu, *Bioinspiration: From Nano to Micro Scales*, Springer, New York, **2012**; b) J. L. Li, X. Y. Liu, *Soft Fibrillar Materials: Fabrication and Applications*, John Wiley & Sons, Berlin, **2013**.
- [2] S. I. Stupp, P. V. Braun, *Science* **1997**, 277, 1242.
- [3] a) Z. Z. Shao, F. Vollrath, *Nature* **2002**, 418, 741; b) G. H. Altman, F. Diaz, C. Jakuba, T. Calabro, R. L. Horan, J. Chen, H. Lu, J. Richmond, D. L. Kaplan, *Biomaterials* **2003**, 24, 401; c) C. Vepari, D. L. Kaplan, *Prog. Polym. Sci.* **2007**, 32, 991.
- [4] a) S. M. Lee, E. Pippel, U. Gosele, C. Dresbach, Y. Qin, C. V. Chandran, T. Brauniger, G. Hause, M. Knez, *Science* **2009**, 324, 488; b) D. H. Kim, J. Viventi, J. J. Amsden, J. L. Xiao, L. Vigeland, Y. S. Kim, J. A. Blanco, B. Panilaitis, E. S. Frechette, D. Contreras, D. L. Kaplan, F. G. Omenetto, Y. G. Huang, K. C. Hwang, M. R. Zakin, B. Litt, J. A. Rogers, *Nat. Mater.* **2010**, 9, 511; c) F. G. Omenetto, D. L. Kaplan, *Nat. Photon.* **2008**, 2, 641; d) A. M. Collins, N. J. V. Skaer, T. Cheysens, D. Knight, C. Bertram, H. I. Roach, R. O. C. Oreffo, S. Von-Aulock, T. Baris, J. Skinner, S. Mann, *Adv. Mater.* **2009**, 21, 75; e) C. J. Bettinger, K. M. Cyr, A. Matsumoto, R. Langer, J. T. Borenstein, D. L. Kaplan, *Adv. Mater.* **2007**, 19, 2847; f) N. C. Tansil, Y. Li, C. P. Teng, S. Y. Zhang, K. Y. Win, X. Chen, X. Y. Liu, M. Y. Han, *Adv. Mater.* **2011**, 23, 1463; g) S. Putthanarat, R. K. Eby, R. R. Naik, S. B. Juhl, M. A. Walker, E. Peterman, S. Ristich, J. Magoshi, T. Tanaka, M. O. Stone, B. L. Farmer, C. Brewer, D. Ott, *Polymer* **2004**, 45, 8451; h) M. Q. Chu, G. J. Liu, *IEEE T. Nano. Tech.* **2008**, 7, 308; i) N. B. Lin, X. Y. Liu, Y. Y. Diao, H. Y. Xu, C. Y. Chen, X. H. Ouyang,

- H. Z. Yang, W. Ji, *Adv. Funct. Mater.* **2012**, 22, 361; j) N. B. Lin, G. W. Toh, Y. Feng, X. Y. Liu, H. Y. Xu, *J. Mater. Chem. B* **2014**, 2, 2136.
- [5] a) M. A. Schreuder, K. Xiao, I. N. Ivanov, S. M. Weiss, S. J. Rosenthal, *Nano Lett.* **2010**, 10, 573; b) A. L. Rogach, N. Gaponik, J. M. Lupton, C. Bertoni, D. E. Gallardo, S. Dunn, N. L. Pira, M. Paderi, P. Repetto, S. G. Romanov, C. O'Dwyer, C. M. S. Torres, A. Eychmuller, *Angew. Chem. Int. Ed.* **2008**, 47, 6538; c) N. Kimura, K. Sakuma, S. Hirafune, K. Asano, N. Hirosaki, R. J. Xie, *Appl. Phys. Lett.* **2007**, 90, 051109; d) R. J. Xie, N. Hirosaki, M. Mitomo, K. Sakuma, N. Kimura, *Appl. Phys. Lett.* **2006**, 89, 241103.
- [6] a) S. F. Wuister, C. de Mello Donegá, A. Meijerink, *J. Am. Chem. Soc.* **2004**, 126, 10397; b) L. Jin, L. Shang, J. Zhai, J. Li, S. Dong, *J. Phys. Chem. C* **2009**, 114, 803.
- [7] a) V. Vohra, G. Calzaferri, S. Destri, M. Pasini, W. Porzio, C. Botta, *ACS Nano* **2010**, 4, 1409; b) H. Z. Sun, H. Zhang, J. H. Zhang, H. T. Wei, J. Ju, M. J. Li, B. Yang, *J. Mater. Chem.* **2009**, 19, 6740; c) H. S. Jang, H. Yang, S. W. Kim, J. Y. Han, S. G. Lee, D. Y. Jeon, *Adv. Mater.* **2008**, 20, 2696; d) M. Strukelj, R. H. Jordan, A. Dodabalapur, *J. Am. Chem. Soc.* **1996**, 118, 1213; e) G. C. Guo, M. S. Wang, W. T. Chen, G. Xu, W. W. Zhou, K. J. Wu, J. S. Huang, *Angew. Chem. Int. Ed.* **2007**, 46, 3909.
- [8] a) N. Hendler, B. Belgorodsky, E. D. Mentovich, M. Gozin, S. Richter, *Adv. Mater.* **2011**, 23, 4261; b) N. Solin, O. Inganäs, *Israel J. Chem.* **2012**, 52, 529.
- [9] J. Kwak, W. K. Bae, M. Zorn, H. Woo, H. Yoon, J. Lim, S. W. Kang, S. Weber, H. J. Butt, R. Zentel, *Adv. Mater.* **2009**, 21, 5022.
- [10] a) N. Du, Z. Yang, X. Y. Liu, Y. Li, H. Y. Xu, *Adv. Funct. Mater.* **2011**, 21, 772; b) B. H. Yang, H. Y. Xu, C. Li, S. Y. Guang, *Chin. Chem. Lett.* **2007**, 18, 960.
- [11] a) F. Lucas, J. Shaw, S. Smith, *Biochem. J.* **1957**, 66, 468; b) J. Warwicker, *Acta Cryst.* **1954**, 7, 565.
- [12] a) X. Wu, X.-Y. Liu, N. Du, G. Xu, B. Li, *Appl. Phys. Lett.* **2009**, 95, 093703; b) N. Du, X. Y. Liu, J. Narayanan, L. A. Li, M. L. M. Lim, D. Q. Li, *Biophys. J.* **2006**, 91, 4528; c) G. Xu, L. Gong, Z. Yang, X.-Y. Liu, *Soft Matter* **2013**; d) X. Hu, D. Kaplan, P. Cebe, *Macromolecules* **2006**, 39, 6161.
- [13] H. Zhang, L. P. Wang, H. M. Xiong, L. H. Hu, B. Yang, W. Li, *Adv. Mater.* **2003**, 15, 1712.
- [14] L.-W. Hsu, Y.-C. Ho, E.-Y. Chuang, C.-T. Chen, J.-H. Juang, F.-Y. Su, S.-M. Hwang, H.-W. Sung, *Biomaterials* **2013**, 34, 784.
- [15] G. D. Kang, J. H. Nahm, J. S. Park, J. Y. Moon, C. S. Cho, J. H. Yeo, *Macromol. Rapid. Comm.* **2000**, 21, 788.
- [16] a) M. M. Coleman, D. J. Skrovanek, J. Hu, P. C. Painter, *Macromolecules* **1988**, 21, 59; b) K. Kunimatsu, B. Bae, K. Miyatake, H. Uchida, M. Watanabe, *J. Phys. Chem. B*, **2011**, 15, 4315.
- [17] M. L. Steigerwald, L. E. Brus, *Accounts. Chem. Res.* **1990**, 23, 183.
- [18] a) W. Liu, M. Howarth, A. B. Greytak, Y. Zheng, D. G. Nocera, A. Y. Ting, M. G. Bawendi, *J. Am. Chem. Soc.* **2008**, 130, 1274; b) E. A. Weiss, R. C. Chiechi, S. M. Geyer, V. J. Porter, D. C. Bell, M. G. Bawendi, G. M. Whitesides, *J. Am. Chem. Soc.* **2008**, 130, 74.
- [19] M. B. M. Susan Sofia, Gloria Gronowicz, David L. Kaplan, *J. Biomed. Mater. Res.* **2001**, 54, 139.